

Improved Resolution of Tertiary Structure Elasticity in Muscle Protein

Jen Hsin and Klaus Schulten*

Department of Physics and Beckman Institute, University of Illinois at Urbana-Champaign, Urbana, Illinois

Supplementary Material

Movies

Movie S1. Movie S1 shows the 100-ns SMD simulation stretching the initially crescent-shaped six-Ig chain into a straight-line conformation with a constant pulling velocity of $v = 1 \text{ \AA/ns}$ (simulation SMD-Ig6-v1 in Table S1). The six Ig domains are colored as defined in Fig. 1A in the main text; the atom fixed during the simulation is shown as a black sphere, while the atom being pulled during the simulation is shown as a gray sphere.

Movie S2. Movie S2 shows the 10-ns SMD simulation stretching the initially crescent-shaped six-Ig chain into a straight-line conformation with a constant pulling velocity of $v = 10 \text{ \AA/ns}$ (simulation SMD-Ig6-v10-1 in Table S1). This simulation has been reported previously in (1) with a further analysis reported here.

Movie S3. Movie S3 shows another 10-ns SMD simulation stretching the initially crescent-shaped six-Ig chain into a straight-line conformation with a constant pulling velocity of $v = 10 \text{ \AA/ns}$ (simulation SMD-Ig6-v10-2 in Table S1); as expected, this trajectory is similar to that of SMD-Ig6-v10-1.

Molecular dynamics protocols

All simulations were carried out with the six-Ig domain segment of the protein titin; the structure of the segment (PDB code 3B43) was reported in (2). The six-Ig structure was solvated in a waterbox large enough for the simulated overall extension, i.e., 100 \AA , and neutralized with 150 mM KCl using plugins in VMD (3).

Equilibrium molecular dynamics. All molecular dynamics simulations were performed with NAMD (4) using the CHARMM27 force field with CMAP correction (5–7) and the TIP3P model for water molecules (8). The equilibrium molecular dynamics simulation (EQ-Ig6 in Table S1) was conducted in the NPT ensemble with the following parameters. Constant temperature at 300 K was maintained using Langevin dynamics with a damping constant of 1 ps^{-1} . Constant pressure of 1 atm was maintained using a Nosé-Hoover Langevin piston barostat (4) with a period of 100 fs and a decay rate of 50 fs. Long-range electrostatic force was computed using the particle-mesh Ewald summation method with a grid size of less than 1 \AA . An integration time step of 1 fs was adopted, with a multiple time-stepping algorithm (9; 10) employed to compute interactions between covalent bonds

every step, short-range non-bonded interactions every other step, and long-range electrostatic forces every four steps.

Steered molecular dynamics. Steered molecular dynamics (SMD) simulations (11) (denoted by “SMD” under the column “Type” in Table S1) were carried out by fixing the N-terminal C_α atom, i.e., the C_α atom of the first residue of I65, while an external force is applied to the C-terminal C_α atom, i.e., to the C_α atom of the last residue of I70, at a constant velocity. For the SMD spring constant a value $k_{\text{SMD}} = 3k_B T / \text{\AA}^2$ was assumed. SMD simulations were carried out in the NVE ensemble, and interactions between covalent bonds, as well as short-range and long-range non-bonded interactions, were computed every timestep, i.e., we adopted so-called ‘1-1-1’ time stepping (12; 13).

Name	Type	Velocity ($\text{\AA}/\text{ns}$)	Atoms	Size (\AA^3)	Time (ns)
SMD-Ig6-v10-1 ¹	SMD	10	276,978	$114 \times 353 \times 72$	10
SMD-Ig6-v10-2 ²	SMD	10	276,978	$114 \times 353 \times 72$	10
SMD-Ig6-v1	SMD	1	276,978	$114 \times 353 \times 72$	100
SMD-Ig6-v0	SMD	0	276,978	$114 \times 353 \times 72$	8
EQ-Ig6 ³	EQ	N/A	223,594	$110 \times 339 \times 63$	25

Table S1: Summary of simulations. Under the column “Type”, SMD denotes constant velocity steered molecular dynamics simulations and EQ denotes equilibrium molecular dynamics simulations.

¹This simulation was performed in (1), with further analysis conducted in the present study.

²This is a repeat simulation, namely, identical to SMD-Ig6-v10-1, carried out for the purpose of sampling; results of this simulation and comparison to simulation SMD-Ig6-v10-1 are discussed below.

³This simulation is an extension from that performed in (1).

Supplemental Data

Here additional results discussed are presented in the form of one table and five figures. Table S2 lists means and variances of the force distributions for fast ($v = 10 \text{\AA}/\text{ns}$; SMD-Ig6-v10-1 in Table S1) and slow ($v = 1 \text{\AA}/\text{ns}$; SMD-Ig6-v1) pulling, as well as those from the simulation with zero pulling velocity (SMD-Ig6-v0). Figures S1-S3 are discussed in the main text. Figure S4 compares two fast pulling simulations (SMD-Ig6-v10-1 and SMD-Ig6-v10-2

in Table S1), the two simulations resulting in similar force-extension relations. Figure S5i shows the angle between all five adjacent Ig pairs as a function of the overall chain extension for all three SMD simulations. Figure S5ii displays the corresponding potential of mean force for the bending motion of each domain pair measured in (1).

	$v = 1 \text{ \AA/ns}$		$v = 10 \text{ \AA/ns}$	
	\bar{F} (pN)	σ_F (pN)	\bar{F} (pN)	σ_F (pN)
$P_f(5\text{\AA})$	16.22	96.36	-12.16	97.12
$P_f(15\text{\AA})$	16.86	99.49	43.29	90.03
$P_f(25\text{\AA})$	0.72	98.42	-2.85	81.89
$P_f(35\text{\AA})$	19.57	91.58	8.00	50.85
$P_f(45\text{\AA})$	28.65	83.25	49.62	74.14
$P_f(55\text{\AA})$	1.86	88.51	95.10	83.76
$P_f(65\text{\AA})$	-8.06	98.51	30.54	59.69
$P_f(75\text{\AA})$	9.15	100.24	35.59	78.24
$P_f(85\text{\AA})$	69.23	104.09	142.49	122.98
$P_f(95\text{\AA})$	166.32	104.12	178.64	76.45

	$v = 0 \text{ \AA/ns}$
P_f	$\bar{F} = 1.01 \text{ pN}; \sigma_F = 92.88 \text{ pN}$

Table S2: Means and variances of force distributions measured in SMD-Ig6-v1, SMD-Ig6-v10-1, and SMD-Ig6-v0, the distributions shown in Fig. 2C of the main text.

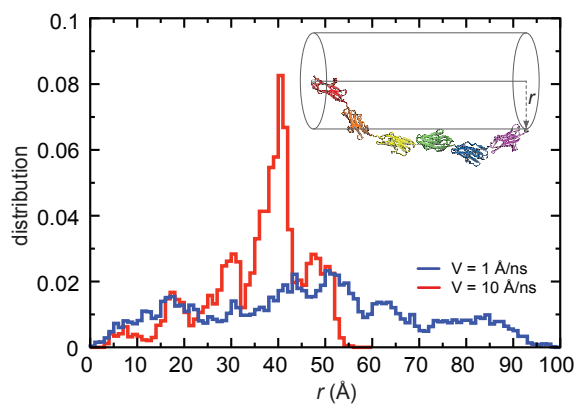


Figure S1: Distribution of the radial position of the pulled atom, i.e., the C_{α} atom of the last residue of I70, in SMD simulations with $v = 10 \text{ \AA/ns}$ (SMD-Ig6-v10-1; red) and $v = 1 \text{ \AA/ns}$ (SMD-Ig6-v1; blue). In the case of slow pulling ($v = 1 \text{ \AA/ns}$), the pulled atom experienced more diffusive motion compared to that in the case of fast pulling ($v = 10 \text{ \AA/ns}$).

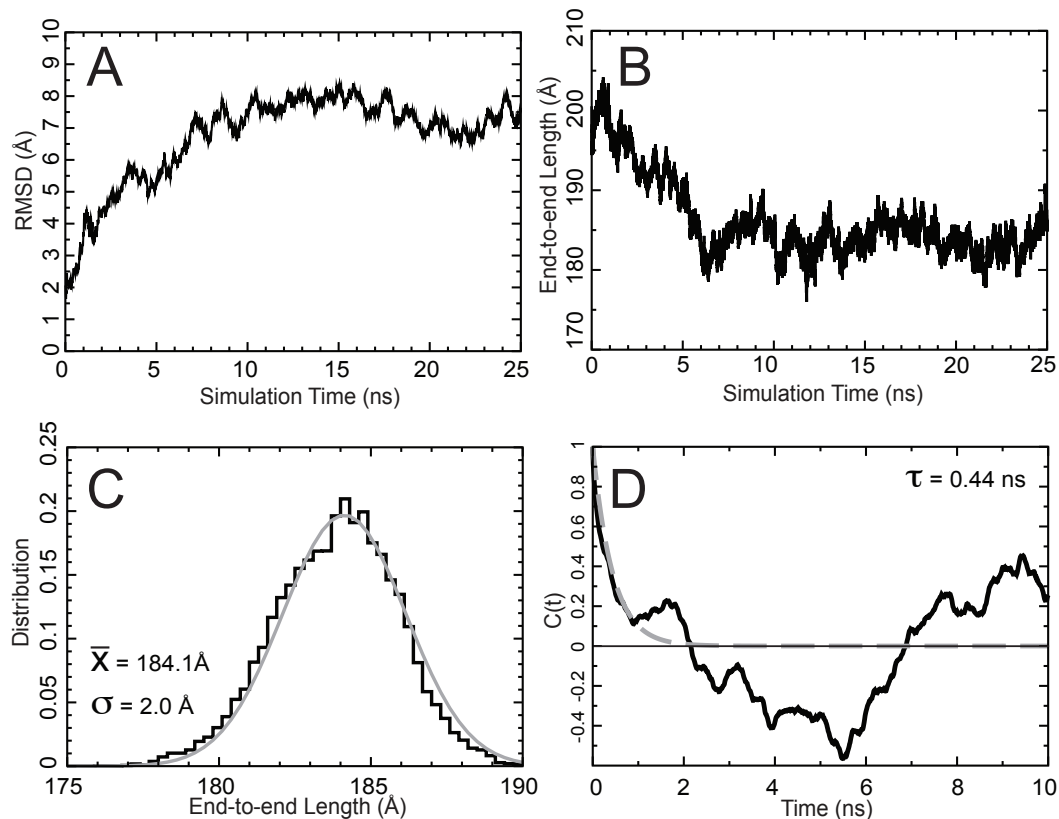


Figure S2: (A) Protein backbone root mean square deviation in reference to the initial structure measured in a 25-ns equilibrium simulation (EQ-Ig6 in Table S1). (B) End-to-end length of the six-Ig chain during the equilibrium simulation. (C) Distribution of the end-to-end length of the six-Ig chain after equilibration was reached. (D) Autocorrelation function of the end-to-end length of the chain (black trace) fitted to a mono-exponential (gray dashed curve).

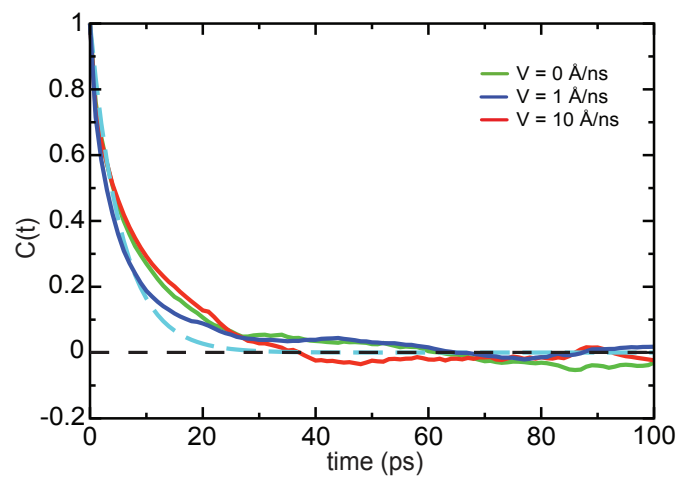


Figure S3: Autocorrelation functions of the stretching force for the three SMD simulations with $v = 0$ (SMD-Ig6-v0; green), 1 (SMD-Ig6-v1; blue), and 10 \AA/ns (SMD-Ig6-v10-1; red). All autocorrelation functions decay nearly exponentially. The mono-exponential fit, $\exp[-t/\tau]$, to the $v = 1 \text{ \AA/ns}$ data is shown as a dashed blue line, which corresponds to a relaxation time constant of $\tau = 5.5 \text{ ps}$.

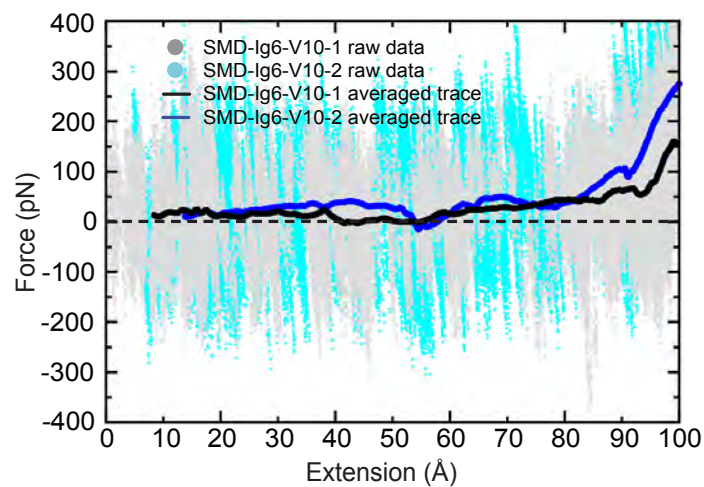


Figure S4: Force-extension relation obtained from the two fast pulling simulations (SMD-Ig6-v10-1 and SMD-Ig6-v10-2). Light blue dots are the raw data from simulation SMD-Ig6-v10-1 reported in (1), and dark blue denotes the averaged trace. Gray dots are the raw data from simulation SMD-Ig6-v10-2, performed in this study, and black denotes the averaged trace. The two averaged traces, although not coinciding at all extension, exhibit the same pattern of low forces during early stretching, with the force rising after 60 Å extension.

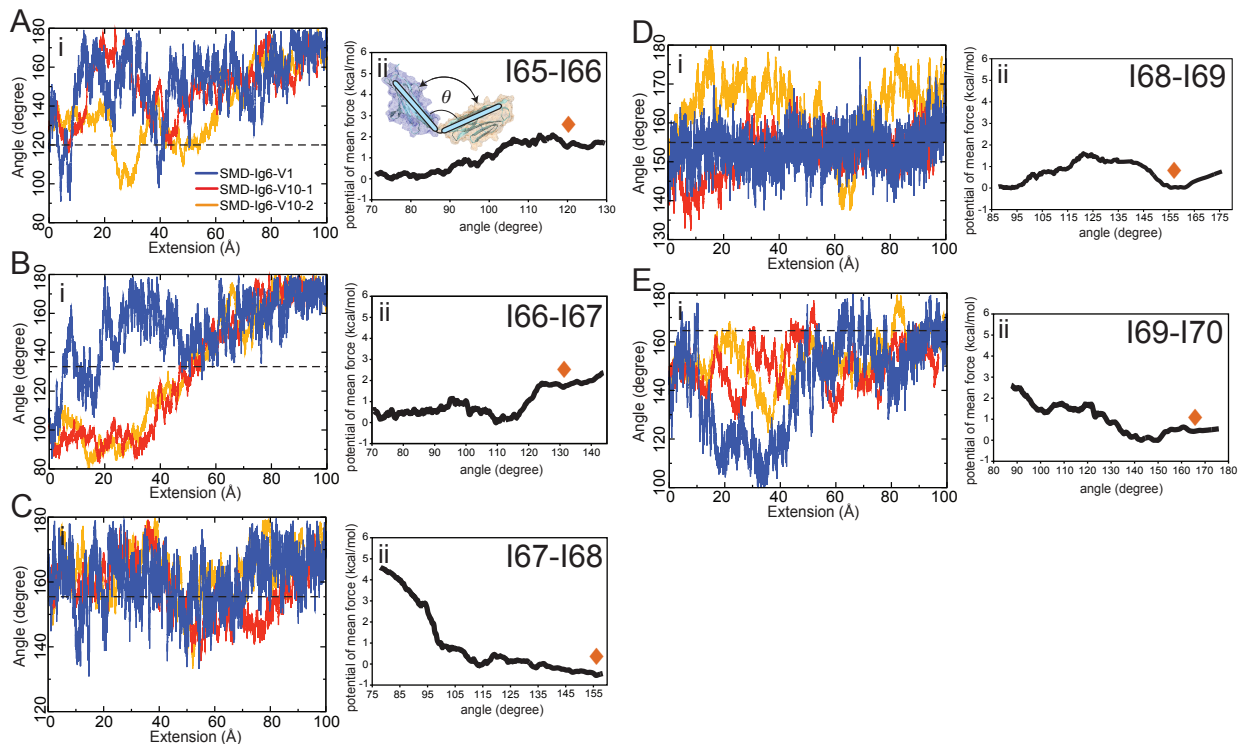


Figure S5: Angles between the five adjacent Ig pairs monitored during all three SMD simulations (SMD-Ig6-v1, SMD-Ig6-v10-1, and SMD-Ig6-v10-2), plotted as a function of overall chain extension. The domain-domain angle is measured using the following procedure: first the principal axes of each domain are measured, and then the angle between the axes with the least moment of inertia from each domain (i.e., the vector around which each domain is the easiest to rotate, this vector should correspond to the longitudinal direction of the domain) is defined to be the domain-domain angle. On the right-hand side of each angle vs. extension plot is the corresponding potential of mean force for the bending degree of freedom as reported in (1), with orange diamonds indicating the equilibrium angles observed. It should be noted that, due to the timescale of the equilibrium molecular dynamics simulations, the equilibrium angles seen in simulations do not always represent the global minimum in the corresponding potential of mean force plots, but rather sometimes land on local energy minima. The only cases where the equilibrium domain-domain angle is also the lowest energy conformation are for the domain pairs I67-I68 (C) and I68-I69 (D). For the former domain pair, the lowest energy state is a fully open conformation, and, as shown in panel C, this domain angle opens up immediately and remains nearly in a fully open state in all three stretching simulations with different velocities. Therefore, domain pair I68-I69 (D) offers the best opportunity to test if the slower stretching velocity preserves the equilibrium domain-domain angle for small extension, as discussed in the main text.

References

- [1] Lee, E. H., J. Hsin, E. von Castelmur, O. Mayans, and K. Schulten. 2010. Tertiary and secondary structure elasticity of a six-Ig titin chain. *Biophys. J.* 98:1085–1095.
- [2] von Castelmur, E., M. Marino, D. I. Svergun, L. Kreplak, Z. Ucurum-Fotiadis, P. V. Konarev, A. Urzhumtsev, D. Labeit, S. Labeit, and O. Mayans. 2008. A regular pattern of Ig super-motifs defines segmental flexibility as the elastic mechanism of the titin chain. *Proc. Natl. Acad. Sci. USA.* 105:1186–1191.
- [3] Humphrey, W., A. Dalke, and K. Schulten. 1996. VMD – Visual Molecular Dynamics. *J. Mol. Graphics.* 14:33–38.
- [4] Phillips, J. C., R. Braun, W. Wang, J. Gumbart, E. Tajkhorshid, E. Villa, C. Chipot, R. D. Skeel, L. Kale, and K. Schulten. 2005. Scalable molecular dynamics with NAMD. *J. Comp. Chem.* 26:1781–1802.
- [5] Mackerell, A. D. 2004. Empirical force fields for biological macromolecules: Overview and issues. *J. Comp. Chem.* 25:1584–1604.
- [6] MacKerell, A. D., Jr., D. Bashford, M. Bellott, R. L. Dunbrack, Jr., J. D. Evanseck, M. J. Field, S. Fischer, J. Gao, H. Guo, S. Ha, D. Joseph, L. Kuchnir, K. Kuczera, F. T. K. Lau, C. Mattos, S. Michnick, T. Ngo, D. T. Nguyen, B. Prodhom, I. W. E. Reiher, B. Roux, M. Schlenkrich, J. Smith, R. Stote, J. Straub, M. Watanabe, J. Wiorcikiewicz-Kuczera, D. Yin, and M. Karplus. 1998. All-atom empirical potential for molecular modeling and dynamics studies of proteins. *J. Phys. Chem. B.* 102:3586–3616.
- [7] Buck, M., S. Bouguet-Bonnet, R. W. Pastor, and A. D. MacKerell. 2006. Importance of the CMAP correction to the CHARMM22 protein force field: Dynamics of hen lysozyme. *Biophys. J.* 90:L36–38.
- [8] Jorgensen, W. L., J. Chandrasekhar, J. D. Madura, R. W. Impey, and M. L. Klein. 1983. Comparison of simple potential functions for simulating liquid water. *J. Chem. Phys.* 79:926–935.
- [9] Grubmüller, H., H. Heller, A. Windemuth, and K. Schulten. 1991. Generalized Verlet algorithm for efficient molecular dynamics simulations with long-range interactions. *Mol. Sim.* 6:121–142.

- [10] Schlick, T., R. Skeel, A. Brünger, L. Kalé, J. A. Board Jr., J. Hermans, and K. Schulten. 1999. Algorithmic challenges in computational molecular biophysics. *J. Comp. Phys.* 151:9–48.
- [11] Isralewitz, B., M. Gao, and K. Schulten. 2001. Steered molecular dynamics and mechanical functions of proteins. *Curr. Opin. Struct. Biol.* 11:224–230.
- [12] Sotomayor, M., D. P. Corey, and K. Schulten. 2005. In search of the hair-cell gating spring: Elastic properties of ankyrin and cadherin repeats. *Structure.* 13:669–682.
- [13] Lee, E. H., J. Hsin, M. Sotomayor, G. Comellas, and K. Schulten. 2009. Discovery through the computational microscope. *Structure.* 17:1295–1306.